SUPPLEMENTAL INFORMATION

Malaria sporozoites traverse host cells within transient vacuoles

Veronica Risco-Castillo, Selma Topçu, Carine Marinach, Giulia Manzoni, Amélie E. Bigorgne, Sylvie Briquet, Xavier Baudin, Maryse Lebrun, Jean-François Dubremetz, Olivier Silvie

Contents:

SUPPLEMENTAL EXPERIMENTAL PROCEDURES

Plasmid constructs

For generation of Py∆*plp1* parasites, a 5' and a 3' fragment of Py*PLP1* gene (PY17X_1007700) were amplified by PCR from *P. yoelii* 17XNL WT genomic DNA, using primers Py*PLP1*rep1for (5'-TCCCCGCGGTCTCTACCTACATATTCAGAAAGAATCC-3'), Py*PLP1*rep2rev (5'-ATAAGAATGCGGCCGCATATTCCACAATTCAATATGCATAAATGCC-3'), Py*PLP1*rep3for (5'-CCGCTCGAGTTGATTATACTACCTTTTTAAGTTGAACC-3') and Py*PLP1*rep4rev (5'-CGGGGTACCAGCAAATAACGATTTATAATTTGTATATCC-3'). The fragments were inserted into *Sac*II/*Not*I and *Xho*I/*Kpn*I restriction sites, respectively, of the GOMO-GFP vector (Manzoni et al., 2014). For generation of Pb∆*plp1* parasites, a 5' and a 3' fragment of Pb*PLP1* gene (PBANKA_100630) were amplified by PCR from *P. berghei* ANKA WT genomic DNA, using primers Pb*PLP1*rep1for (5'-TCCCCGCGGAAATTGAAAAATAAGTTTGGCTAGTTACAC-3'), Pb*PLP1*rep2rev (5'-ATAAGAATGCGGCCGCGTATCAAAAAATCTTTATTGCACATTCCAC-3'), Pb*PLP1*rep3for (5'-CCGCTCGAGAGGCATGAAAAGTTGTTCGCTAAATATGG-3') and Pb*PLP1*rep4rev (5'-GGGGTACCTAACGCGGAATCTGCAAGGTATATCG-3'). The fragments were inserted into *Sac*II/*Not*I and *Xho*I/*Kpn*I restriction sites, respectively, of the GOMO-GFP vector (Manzoni et al., 2014). The resulting targeting constructs were verified by DNA sequencing (GATC Biotech), and were linearized with *Sac*II and *Kpn*I before transfection. The plasmid construct used for mCherry tagging of PyRON4 (PY17X_0934000) has been described previously (Risco-Castillo et al., 2014).

Parasite transfection and selection

For double crossover replacement of *PLP1* gene and generation of the Py∆*plp1* and Pb∆*plp1* parasite lines, purified schizonts of wild type *P. yoelii* 17XNL or *P. berghei* ANKA were transfected with 5-10 µg of linearized construct by electroporation using the AMAXA Nucleofector™ device (program U33), as described elsewhere (Janse et al., 2006), and immediately injected intravenously in the tail of one mouse. The day after transfection,

pyrimethamine (7 or 70 mg/L for *P. yoelii* and *P. berghei*, respectively) was administrated in the mouse drinking water, for selection of transgenic parasites. Pure transgenic parasite populations were isolated by flow cytometry-assisted sorting of GFP and mCherry-expressing blood stage parasites FACSAria II (Becton-Dickinson), transferred into naïve mice, treated with 1 mg/ml 5-fluorocytosine (Meda Pharma) in the drinking water, and sorted again for selection of GFP+ parasites only, as described (Manzoni et al., 2014). Parasite genomic DNA was extracted using the Purelink Genomic DNA Kit (Invitrogen), and analysed by PCR using primer combinations specific for WT and recombined loci. For genotyping of Py∆*plp1* parasites, we used primer combinations specific for the WT Py*PLP1* locus (5'-TGATATTCTCTTTGGAAATCCATTAGGAG-3' and 5'-TACACTTACTCCATCTTTTTTCATTTGG-3'), for the 5' region of the recombined locus (5'-TCTGCAGTGTCACCTATGTTTTCAGG-3' and 5'-TAATAATTGAGTCTTTAGTAACGAATTGCC-3'), and for the 3' region of the recombined locus before (5'-ATCGTGGAACAGTACGAACGCGCCGAGG-3' and 5'-AGCTATACGATACGTCTACATGGGTTCTC-3') or after excision of the selectable marker (5'-GATGGAAGCGTTCAACTAGCAGACC-3' and 5'-AGCTATACGATACGTCTACATGGGTTCTC-3'). For genotyping of Pb∆*plp1* parasites, we used primer combinations specific for the WT Pb*PLP1* locus (5'-TTATAAACTCCCTGCGTATCTCAGTTCGC-3' and 5'-TCATCTGTATCTGATTCATCATCATCACC-3'), for the 5' region of the recombined locus (5'-ATCCACAAGTTTTTACCCAATTTATTGG-3' and 5'-TAATAATTGAGTCTTTAGTAACGAATTGCC-3'), and for the 3' region of the recombined locus before (5'-ATCGTGGAACAGTACGAACGCGCCGAGG-3' and 5'-AAACACATCATCCCTAAAGAAGTTAAACC-3') or after excision of the selectable marker (5'-GATGGAAGCGTTCAACTAGCAGACC-3' and 5'-AAACACATCATCCCTAAAGAAGTTAAACC-3'). Genotyping of Py*PLP1*/RON4::mCherry parasites was performed as described for PyGFP/RON4::mCherry parasites (Risco-Castillo et al., 2014).

Live imaging of sporozoite gliding motility and cell traversal

Imaging of gliding sporozoites was performed at 37°C, with GFP images being recorded every 3 seconds during 3 minutes, using a Zeiss Axio Observer.Z1 inverted fluorescence microscope equipped with a N-Achroplan 10x/0.25 Ph1 M27 objective. To visualize CT events, HepG2 cells were incubated at 37°C with GFP-expressing sporozoites in the presence of 10 µg/ml propidium iodide (P-3566, Life technologies), as described (Formaglio et al., 2014). GFP, propidium iodide and transmitted light images were recorded every 5 min during 1 hour, at 37°C, using a LD Plan-Neofluar 40X/0.6 Corr Ph2 M27 objective.

***In vivo* experiments**

To analyze blood stage growth, groups of Swiss mice (n = 5) were injected intravenously with 1 x 10^4 PyGFP- or Py∆*plp1*-infected erythrocytes. Parasitemia was then followed daily for three weeks using a Guava EasyCyte flow cytometer (Millipore). To determine sporozoite infectivity *in vivo*, groups of BALB/c mice (n = 4 or 5 per group) were injected intravenously with 1 x 10^4 sporozoites of PyGFP, Py∆*plp1* or WT *P. yoelii* parasites, or exposed to the bite of 20 infected mosquitoes. Mice were then followed daily by FACS for the appearance of blood stage parasites.

Supplemental References

Formaglio, P., Tavares, J., Menard, R., and Amino, R. (2014). Loss of host cell plasma membrane integrity following cell traversal by Plasmodium sporozoites in the skin. Parasitol Int *63*, 237–244.

Janse, C.J., Ramesar, J., and Waters, A.P. (2006). High-efficiency transfection and drug selection of genetically transformed blood stages of the rodent malaria parasite Plasmodium berghei. Nat Protoc *1*, 346–356.

Manzoni, G., Briquet, S., Risco-Castillo, V., Gaultier, C., Topcu, S., Ivanescu, M.L., Franetich, J.F., Hoareau-Coudert, B., Mazier, D., and Silvie, O. (2014). A rapid and robust selection procedure for generating drug-selectable marker-free recombinant malaria parasites. Sci Rep *4*, 4760.

Mueller, A.K., Camargo, N., Kaiser, K., Andorfer, C., Frevert, U., Matuschewski, K., and Kappe, S.H. (2005). Plasmodium liver stage developmental arrest by depletion of a protein at the parasite-host interface. Proc Natl Acad Sci U S A *102*, 3022–3027.

Risco-Castillo, V., Topcu, S., Son, O., Briquet, S., Manzoni, G., and Silvie, O. (2014). CD81 is required for rhoptry discharge during host cell invasion by Plasmodium yoelii sporozoites. Cell Microbiol *16*, 1533–1548.

Silvie, O., Franetich, J.F., Boucheix, C., Rubinstein, E., and Mazier, D. (2007). Alternative invasion pathways for Plasmodium berghei sporozoites. Int J Parasitol *37*, 173–182.

Silvie, O., Briquet, S., Muller, K., Manzoni, G., and Matuschewski, K. (2014). Post-transcriptional silencing of UIS4 in Plasmodium berghei sporozoites is important for host switch. Mol Microbiol *91*, 1200–1213.

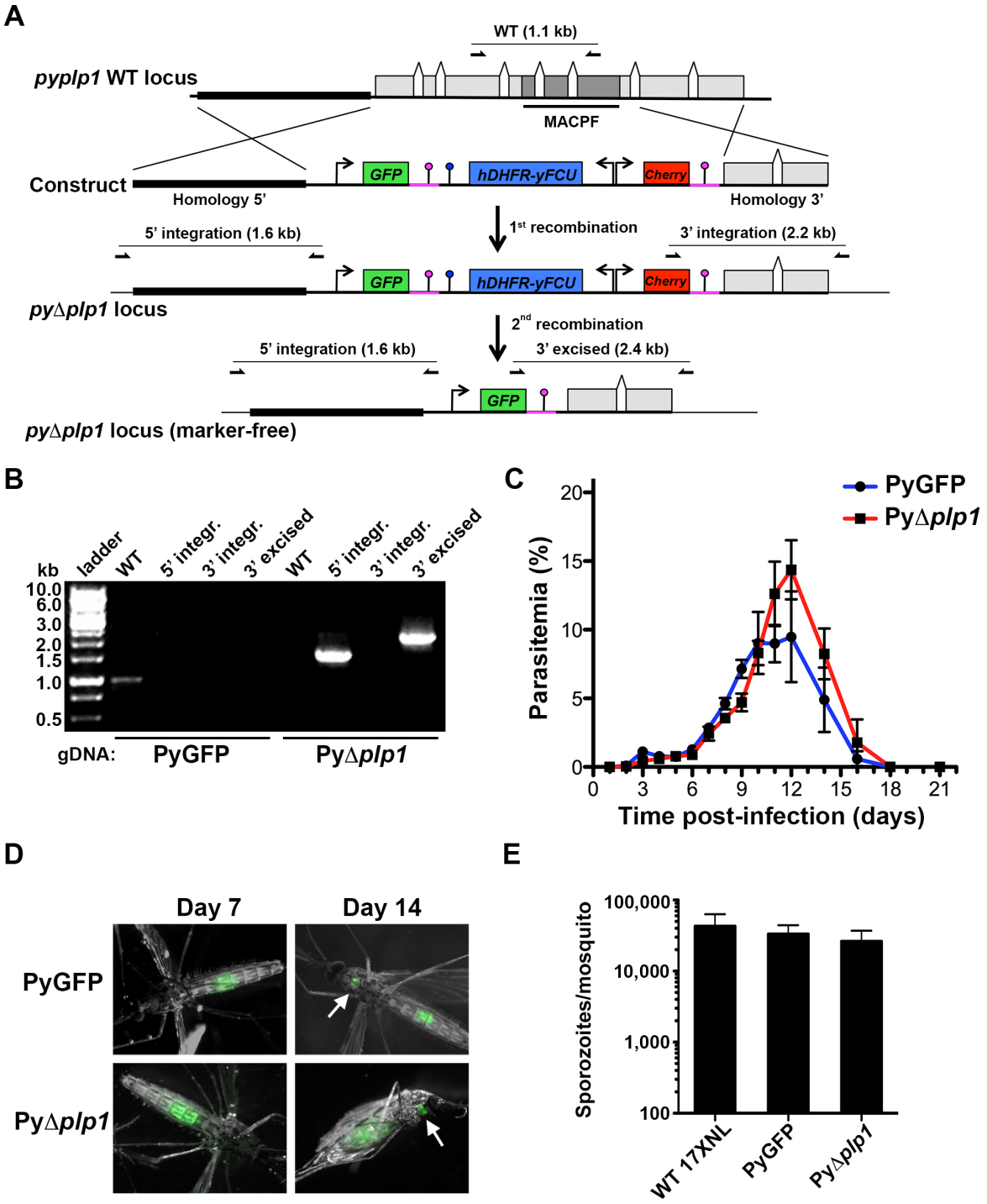

Figure S1, related to Figure 3. Targeted gene deletion of *plp1* in *P. yoelii*. A. Replacement strategy to generate PyΔ*plp1*. The wild-type (WT) genomic locus of *P. yoelii plp1* was targeted with a GOMO-GFP replacement plasmid containing a 5' and a 3' homologous sequence inserted on each side of the plasmid GFP/hDHFR-yFCU/mCherry triple cassette. Upon double crossover recombination, the *plp1* gene is replaced by the plasmid cassettes. Subsequent recombination between the two identical PbDHFR/TS 3' UTR sequences (pink lollipops) results in excision of hDHFR-yFCU and mCherry. Genotyping

primers and expected PCR fragments are indicated by arrows and lines, respectively. B. PCR analysis of genomic DNA isolated from control PyGFP and Py∆*plp1* parasites recovered after GOMO selection. Confirmation of the predicted recombination events was achieved with primer combinations specific for 5' integration (5' integr.) or 3' integration followed by marker excision (3' excised). Primers used for genotyping are indicated in the Supplemental Experimental Procedures. The absence of amplification with primer combinations specific for the WT locus (WT) and the non-excised integrated construct (3' integration) confirms that the final populations contain only Py∆*plp1* drug-selectable marker-free *P. yoelii* parasites. C. Swiss mice (n = 5) were injected intravenously with 1 x 10^4 PyGFP- or Py∆*plp1*-infected erythrocytes. Parasitemia was then followed by FACS for 3 weeks. P > 0.05 (Two-way ANOVA followed by Bonferroni test). D. Fluorescence imaging of whole mosquitoes infected with PyGFP or Py∆*plp1* parasites, day 7 and day 14 after the infectious blood meal. The mosquito salivary glands are indicated with arrows. E. Parental WT (17XNL), PyGFP and Py∆*plp1* parasites were transmitted to female *A. stephensi* mosquitoes. The mean number of salivary gland sporozoites per mosquito was determined 14 days after mosquito infection. Results are expressed as the mean value (± SD) from at least six independent experiments. P > 0.16 (Kruskal–Wallis test).

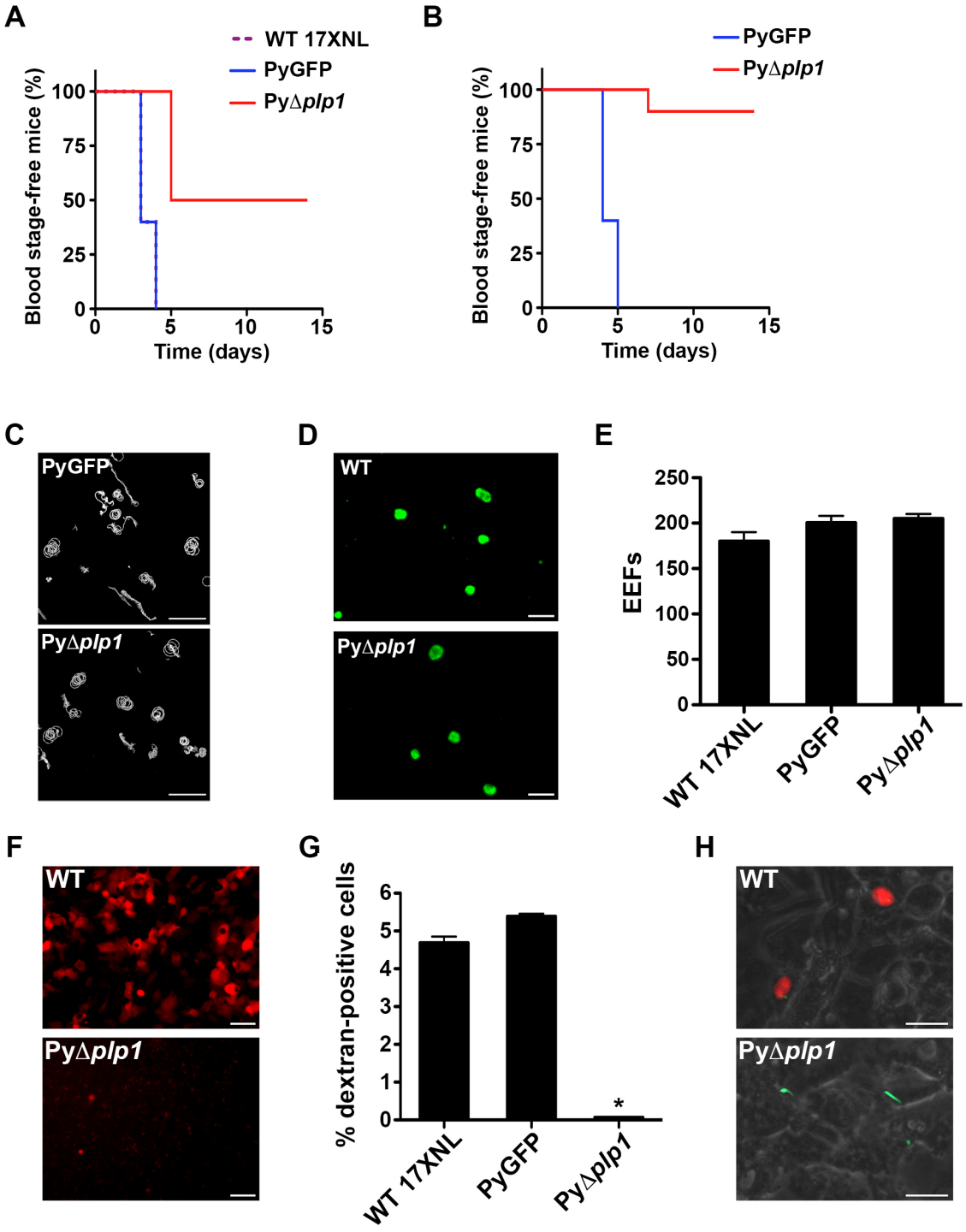

Figure S2, related to Figure 3. PLP1 is required for *P. yoelii* sporozoite cell traversal. A. Kaplan-Meier analysis of time to patency in BALB/c mice (n = 4 or 5 per group) after intravenous injection of 10^4 PyGFP, PyΔ*plp1* or WT *P. yoelii* sporozoites. Mice were followed daily for the appearance of blood stage parasites. P = 0.099 (Log rank Mantel-Cox test). B. Kaplan-Meier analysis of time to patency in BALB/c mice exposed to the bites of 20 mosquitoes infected with PyGFP (n = 5) or PyΔ*plp1* (n = 10) parasites. Mice were followed daily by FACS for the appearance of blood stage parasites. Shown are cumulative results of two independent experiments. P < 0.0001 (Log rank Mantel-Cox test). C. Gliding motility of

PyGFP and PyΔ*plp1* sporozoites. Shown are the maximum intensity projections of 0-180 seconds time-series acquisition of GFP fluorescence from Supplemental Movies S4 and S5, respectively. Bars, 100 µm. D. HepG2/CD81 cells were incubated with parental (WT 17XNL) or PyΔ*plp1* sporozoites for 48 h before immunofluorescence labelling of exo-erythrocytic forms (EEFs) with anti-HSP70 antibodies (green). Bars, 50 µm. E. Quantification of liver-stage development in cultured hepatoma cells. HepG2/CD81 cells (5×10^4) were infected with parental (WT 17XNL), PyGFP or PyΔ*plp1* sporozoites (5×10^3). The number of EEFs in triplicate wells was determined 48 h post infection. $P > 0.05$ (Kruskal–Wallis test). F. HepG2/CD81 cells were incubated with parental (WT 17XNL) or PyΔ*plp1* sporozoites for 3 h in the presence of rhodamine-labelled dextran (red), fixed and examined by fluorescence microscopy. Bars, 50 µm. G. HepG2/CD81 cells (5×10^4) were incubated for 1 h with parental (WT 17XNL), PyGFP or PyΔ*plp1* sporozoites (5×10^3) in the presence of rhodamine-labelled dextran. The percentage of traversed (dextran-positive) cells was determined in triplicate wells by FACS. * $p < 0.05$ (Kruskal–Wallis test). H. HepG2 cells were incubated for 1 h with PyGFP or PyΔ*plp1* sporozoites (green) in the presence of propidium iodide (red), which labels the nucleus of traversed cells. Images were extracted from Supplemental Movies S6 and S7. Bars, 20 µm.

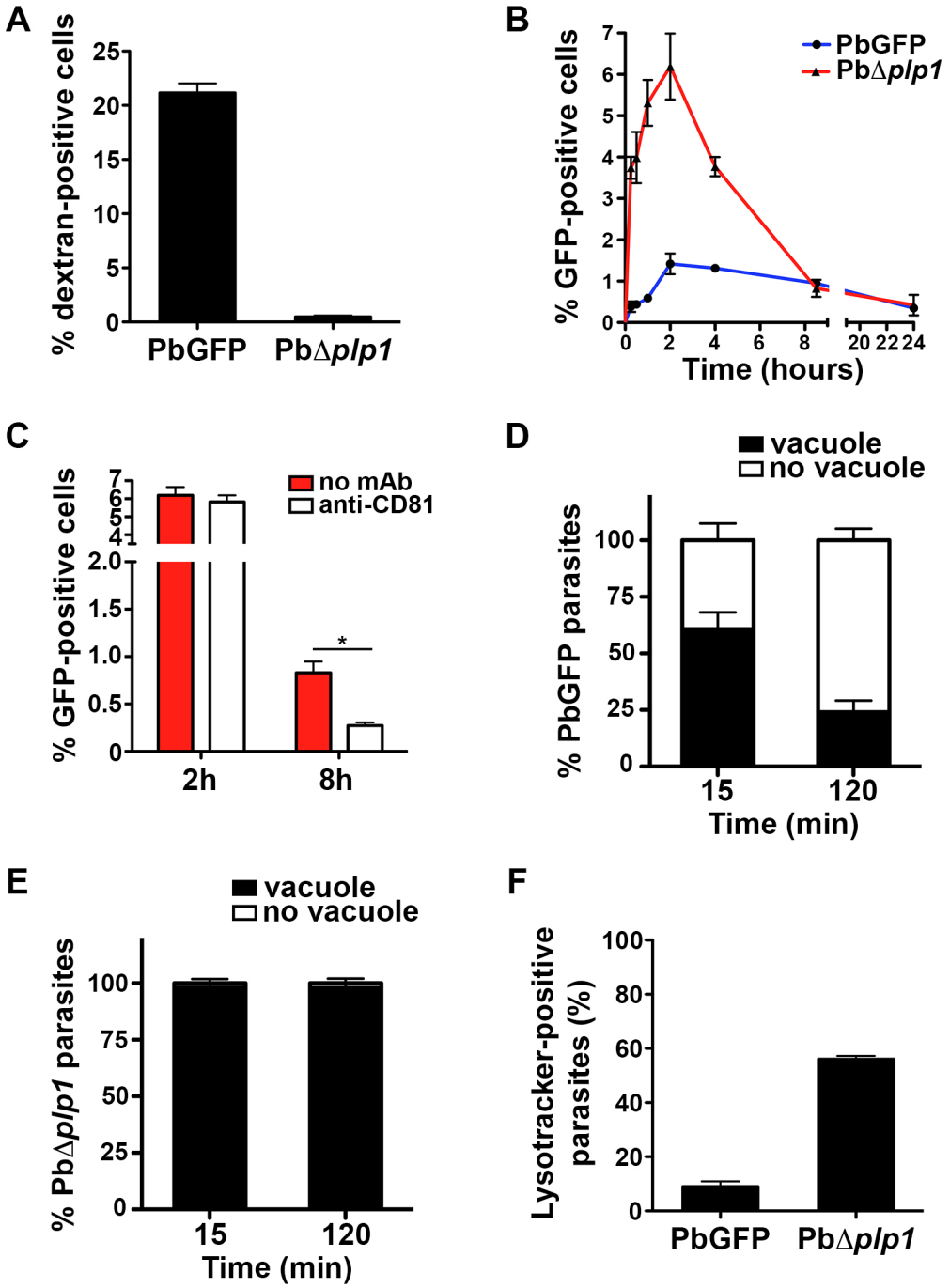

Figure S3, related to Figure 3. *P. berghei* sporozoites use PLP1 to egress from transient vacuoles. In order to confirm that PLP1-dependent sporozoite egress occurs in other *Plasmodium* species, we performed experiments with *plp1*-deficient *P. berghei* parasites, generated with the GOMO strategy, using PbGFP parasites as control parasites (Manzoni et al., 2014) (A). For these experiments, we used the mouse hepatoma cell line Hepa1-6, where *P. berghei* infection depends on CD81 (Silvie et al., 2007). Invasion of Hepa1-6 cells by PbΔ*plp1* sporozoites occurred earlier and at a higher rate as compared to PbGFP parasites, but the number of parasites decreased beyond 2 hours, resulting in identical infection rates between PbGFP and PbΔ*plp1* parasites after 8 hours (B). Antibodies against CD81 had no effect on the early invasion events but inhibited productive invasion of

PbΔ*plp1* sporozoites (C). Invasion assays performed in Hepa1-6/N20-mCherry cells in the presence of anti-CD81 antibodies revealed that a large proportion of PbGFP were contained inside a vacuole at early time points (D), showing that *P. berghei* sporozoites, like *P. yoelii*, form TVs during CT. As expected, all intracellular PbΔ*plp1* sporozoites were localized inside a vacuole (E). These results show that CT-deficient *P. berghei*, like the *P. yoelii* mutants, predominantly form non-replicative vacuoles independently of host entry factors, and confirm the role of PLP1 in sporozoite egress from TVs. A. Hepa1-6 cells (5 x 10^4) were incubated for 2 h with PbGFP or PbΔ*plp1* sporozoites (5 x 10^3) in the presence of rhodamine-labelled dextran. The percentage of traversed (dextran-positive) cells was determined in triplicate wells by FACS. B. Hepa1-6 cells (5 x 10^4) were incubated with PbGFP or PbΔ*plp1* sporozoites (1 x 10^4) for up to 24 h, and analysed by FACS to determine the percentage of infected (GFP-positive) cells. C. Hepa1-6 cells (5 x 10^4) were incubated with PbΔ*plp1* sporozoites (1 x 10^4) for 2 or 8 h, in the presence or absence of anti-CD81 antibodies, and analysed by FACS to determine the percentage of infected (GFP-positive) cells. *, $p = 0.05$ (Mann-Whitney U test). D. Hepa1-6/N20-mCherry cells were incubated with PyGFP sporozoites in the presence of anti-CD81 antibodies for 15 or 120 min before fixation and labeling with filipin, and the presence or absence of a vacuole was determined by fluorescence microscopy. E. Hepa1-6/N20-mCherry cells were incubated with PbΔ*plp1* sporozoites in the presence of anti-CD81 antibodies for 15 or 120 min before fixation and labeling with filipin, and the presence or absence of a vacuole was determined by fluorescence microscopy. F. Hepa1-6 cells were incubated with PbGFP or PbΔ*plp1* sporozoites for 4 h, labelled with Lysotracker-red and analysed by fluorescence microscopy to determine the proportion of Lysotracker-positive parasites among intracellular PbGFP (n = 56) and PbΔ*plp1* parasites (n = 75).

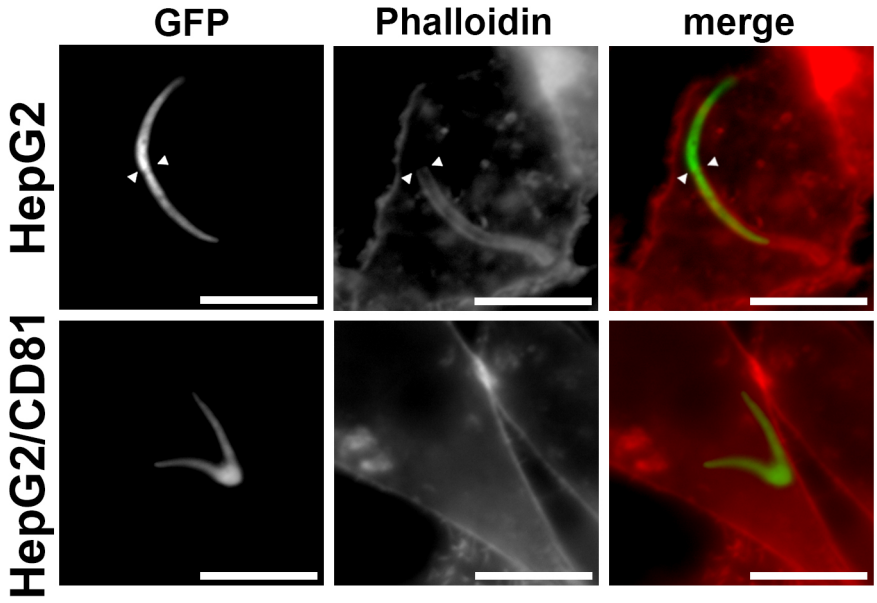

Figure S4, related to Figure 4. Phalloidin labels transient vacuoles but not PVs. HepG2 and HepG2/CD81 cells were incubated for 15 or 120 min, respectively, with PyGFP sporozoites, fixed, and labeled with phalloidin-TRITC. The upper panels show a sporozoite egressing from a phalloidin-labeled vacuole; the arrowheads indicate where the vacuole was ruptured. Bars, 10 μm.

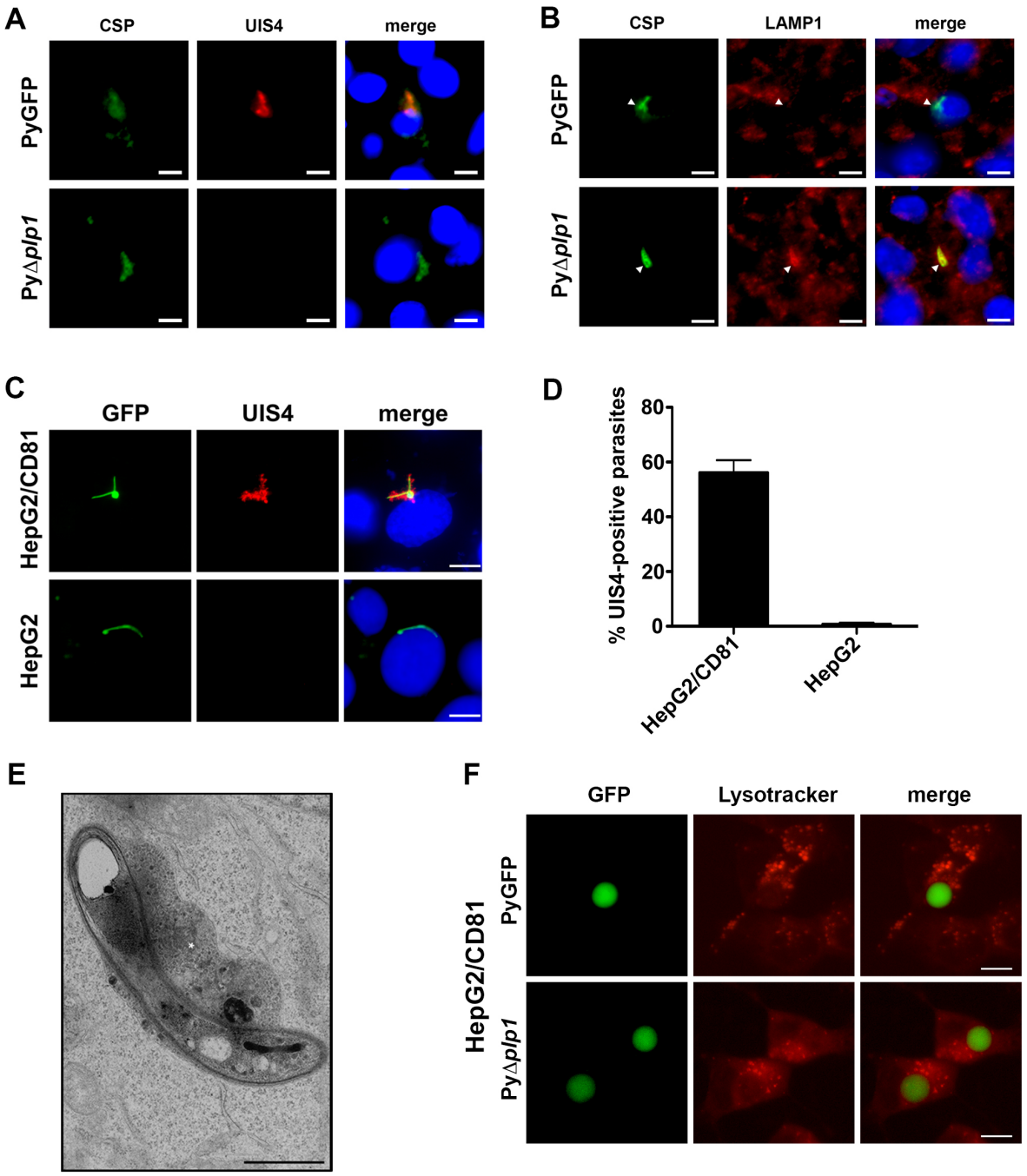

Figure S5, related to Figure 5. Non-replicative PyΔ*plp1* vacuoles are targeted by the host cell lysosomes. A-B. PLP1-deficient *P. yoelii* vacuoles are targeted by the host cell lysosomes *in vivo*. Immunofluorescence analysis of liver sections from BALB/c mice infected with PyGFP or PyΔ*plp1* sporozoites. Samples were fixed 3 hours post-infection, and labelled with antibodies against CSP (green) and either UIS4 (A, red) or LAMP1 (B, red). Nuclei were stained with Hoechst 33342 (blue). Bars, 5 µm. C-D. UIS4 is expressed in the membrane of PVs but not TVs. GFP-expressing PyΔ*plp1* sporozoites were incubated with HepG2 or HepG2/CD81 cells for 4 hours, then fixed and analyzed by immunofluorescence using anti-UIS4 antibodies (red). Nuclei were stained with Hoechst 33342 (blue). Scale bars, 10 µm. Panel D indicates the proportion of parasites expressing UIS4 among infected cells (mean +/- SD). After host cell invasion, the parasite normally remodels the PVM by inserting parasite-derived proteins such as UIS4 (Mueller et al., 2005; Silvie et al., 2014). UIS4 was not detected in non-replicative vacuoles formed by PyΔ*plp1* sporozoites inside HepG2 cells. In HepG2/CD81 cells, only a fraction of PyΔ*plp1* intracellular parasites expressed UIS4,

consistent with both types of vacuoles being formed in these cells. E. TEM image of a PyΔ*plp1* sporozoite inside an infected HepG2 cell, 5 h post-infection. Note the accumulation of granular material in the parasite vacuole. Bar, 1 μm. F. *P. yoelii* EEFs avoid fusion with the host cell lysosomes. HepG2/CD81 cells were incubated with GFP-expressing PyGFP or PyΔ*plp1* sporozoites for 24 hours before labelling with the Lysotracker-red reagent and live fluorescence imaging. Bars, 10 μm.

SUPPLEMENTAL MOVIES

Movie S1, related to Figure 2. Spinning disk confocal microscopy of HepG2/N20-mCherry cells, showing egress of a PyGFP sporozoite (green) from a N20-mCherry-labeled vacuole (red). Sporozoite egress occurs at 25 seconds, and is followed by vacuole collapse. Bars, 10 µm.

Movie S2, related to Figure 2. Spinning disk confocal microscopy of HepG2/N20-mCherry cells, showing egress of a PyGFP sporozoite (green) from a N20-mCherry-labeled vacuole (red). Sporozoite egress occurs between 144 and 154 seconds. Bars, 10 µm.

Movie S3, related to Figure 3. Spinning disk confocal microscopy of a Py∆*plp1* sporozoite (green) in a HepG2/N20-mCherry cell (membranes labeled in red). Note that the parasite remains inside a N20-mCherry-labeled vacuole during the entire duration of the movie. Bars, 10 µm.

Movie S4, related to Figure 3. Gliding motility of PyGFP sporozoites. Time labels are expressed in seconds.

Movie S5, related to Figure 3. Gliding motility of Py∆*plp1* sporozoites. Time labels are expressed in seconds.

Movie S6, related to Figure 3. Movie showing PyGFP sporozoite cell traversal activity. GFP-expressing PyGFP sporozoites (green) were incubated with HepG2 cells in the presence of propidium iodide (red), which labels the nucleus of cells with altered plasma membrane integrity. Time labels are expressed in minutes.

Movie S7, related to Figure 3. Movie showing Py∆*plp1* sporozoites (green) incubated with HepG2 cells in the presence of propidium iodide (red). Incorporation of propidium iodide in the host cell nucleus was not observed with Py∆*plp1* sporozoites, consistent with abrogation of cell traversal activity. Time labels are expressed in minutes.